Arch. Metall. Mater. **64** (2019), 2, 513-518

DOI: 10.24425/amm.2019.127569

TAE-HOON KANG*, KYU-SIK KIM*, MAN-HO PARK**, KEE-AHN LEE*#

HIGH TEMPERATURE RANDOM STACK CREEP PROPERTY OF Ni-Cr-Al BASED POWDER POROUS METAL MANUFACTURED WITH POWDER SINTERING PROCESS

Recently, attempts have been made to use porous metal as catalysts in a reactor for the hydrogen manufacturing process using steam methane reforming (SMR). This study manufactured Ni-Cr-Al based powder porous metal, stacked cubic form porous blocks, and investigated high temperature random stack creep property. To establish an environment similar to the actual situation, a random stack jig with a 1-inch diameter and height of 75 mm was used. The porous metal used for this study had an average pore size of ~1161 μm by rolling direction. The relative density of the powder porous metal was measured as 6.72%. A compression test performed at 1073K identified that the powder porous metal had high temperature (800°C) compressive strength of 0.76 MPa. A 800°C random stack creep test at 0.38 MPa measured a steady-state creep rate of 8.58×10^{-10} s^{-1}, confirming outstanding high temperature creep properties. Compared to a single cubic powder porous metal with an identical stress ratio, this is a 1,000-times lower (better) steady-state creep rate. Based on the findings above, the reason of difference in creep properties between a single creep test and random stack creep test was discussed.

Keywords: powder porous metal, high-temperature, compression test, creep property

1. Introduction

Metal foam (porous metal) refers to structures that are composed of numerous small cells in a regular or irregular distribution, and 15-95% of their volume consists of pore structures. Metal foam is more lightweight and has greater surface area compared to bulk materials. In addition, it has outstanding specific weight capacity of energy absorption and fluid permeability. Therefore, it is commonly used in shock absorbers, filters and heat exchangers [1-4]. There have been many studies recently investigating the possibility of using the large surface areas of metal foam materials as catalyst supporters [5-7].

Ni-based superalloy is an alloy known to have outstanding mechanical properties, oxidation resistance, corrosion and creep resistances at high temperatures [8]. Therefore, it is commonly used as a material for components exposed to high temperature environments such as aircraft jet engines and turbine blades. For this reason, there have been many attempts to manufacture metal foam using Ni-based superalloy. Recently, a powder alloying process was developed to manufacture metal foam using Ni-based super heat-resistant alloy [9]. This powder alloying process can manufacture Ni superalloy porous metal by applying alloying powder to pure Ni foam and then applying heat treatment. This process can easily control the chemical composition according to the type of alloy powder and spraying amount, and it can also control the shape and surface area of the porous metal according to an initial polyurethane pre-form shape. The authors of this study have reported the high temperature oxidation [10] and creep property [11] of Ni-Fe-Cr-Al porous metal manufactured using this process.

Meanwhile, porous materials used as the filter, plant and catalyst for reactors and are manufactured in small sizes to achieve ease of replacement and cost reduction, and they are used in stacking condition for extended periods of time. This leads to the porous material being exposed to multiaxial stress due to random stacking. Therefore, it is necessary to investigate high temperature creep properties, which can forecast the life endurance using time-dependent properties. However, there is no study that investigated the mechanical properties of metal foam at high temperatures in conditions simulating the environment where actually it is used.

Therefore, this study has implemented a random stack creep test using a superalloy foam cube with Ni-Cr-Al composition. With the test, this study investigated the creep property of Ni-based superalloy foam in actual conditions where it is used as filter or catalyst, and analyzed its creep behavior.

2. Experimental Method

The porous metal used in this study was manufactured by Alantum Co. Ltd., spraying Ni-Cr-Al alloy powder to a pure Ni foam sheet and then performing debinding and sintering pro-

* DEPARTMENT OF MATERIALS SCIENCE AND ENGINEERING, INHA UNIVERSITY, INCHEON 22212, REPUBLIC OF KOREA
** ASFLOW CO. LTD., HWASEONG 18522, REPUBLIC OF KOREA
# Corresponding author: keeahn@inha.ac.kr

cesses. To fabricate cube form, two manufactured sheets were stacked and underwent high temperature rolling to a bulk type foam. Then, the material was cut into a 10 mm×10 mm×10 mm cube form. XRF (X-ray fluorescence spectrometer, ZSX Primus II) analysis results of the Ni-Cr-Al porous metal represented the chemical composition of Ni-14.7%Cr-16.5%Al (wt.%).

SEM (scanning electron microscopy, VEGA II LMU) was used to measure pore size and perform microstructural observation. An image analysis program was used to calculate the average pore size. ND (normal direction), TD (transverse direction) and RD (rolling direction) SEM images were used for the calculation. A typical microstructure analysis method was used to observe the microstructure. Silicon carbide papers (#100 ~ #2000) and 1 μm alumina slurry was used for micro-polishing. Then, the material was etched in 5 ml acetic acid + 10 ml HNO_3 + 85 ml water solution, and the microstructure of the strut was observed. X-ray diffractometer (XRD, Ultima IV) was used for phase analysis. In addition, an electron probe microscope (EPMA, Shimadzu, EPMA-1600) was used to identify the alloying element distribution.

Room and high temperature compression tests of a single cubic Ni-Cr-Al foam were performed using MTS-810 equipment. For a high temperature compression test, the temperature was increased at a rate of 5 °C/min. up to 800°C. Regardless of compression test temperature, the initial strain rate was set as 1×10^{-3} /s, and tests were performed until total strain (ε_t) = 0.6. In addition, to identify anisotropy, compression tests were performed in ND and RD.

A high temperature random stacking creep test was performed using an RB-306 DW direct creep tester. A random creep jig, as depicted in Fig. 1, with a diameter of 25.4 mm and × height of 75 mm was built to perform the simulated test of actual reactors. Furnace was installed in the chamber that surrounds the creep jig. Thermocouples with a temperature error of ±1°C were attached on the top, middle, and bottom of the creep jig, allowing temperature to be checked and stored in seconds. The creep test was performed with 16 cubic porous metals used in this study

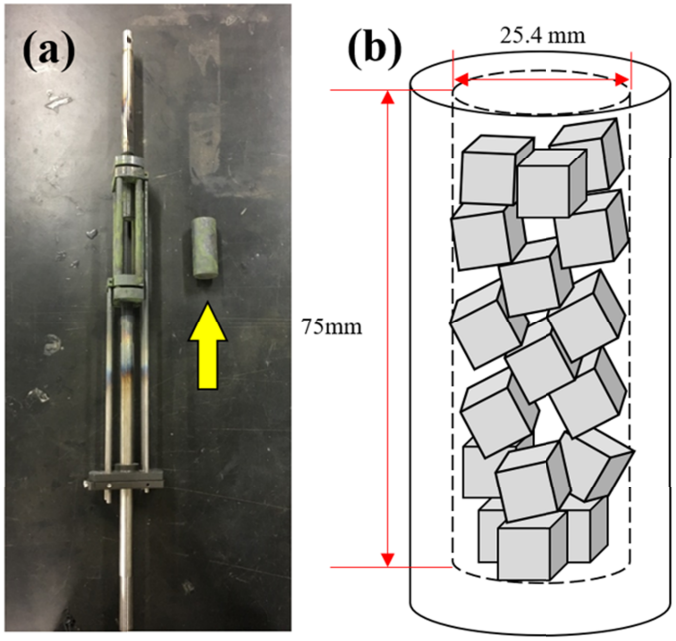

Fig. 1. Macro images of (a) random stack creep test jig and (b) description of random stacked Ni-Cr-Al specimens in jig

inserted in the creep jig. A test pressure of 0.114 ~ 0.38 MPa was applied based on the single high temperature compression property of the Ni-Cr-Al porous metal. The initial temperature was increased up to 800°C with a 5°C/min. temperature increase rate, and the creep strain was measured for 48 hours. The load during the high temperature compression creep test was a constant load type, and an extensometer capable of detecting changes up to 0.001 mm was used to analyze changes in the specimen.

3. Results and discussion

The pores of the Ni-Cr-Al powder porous metal were observed using SEM, and the results are shown in Fig. 2(a). The pores had a three-dimensional net formation. The pore size,

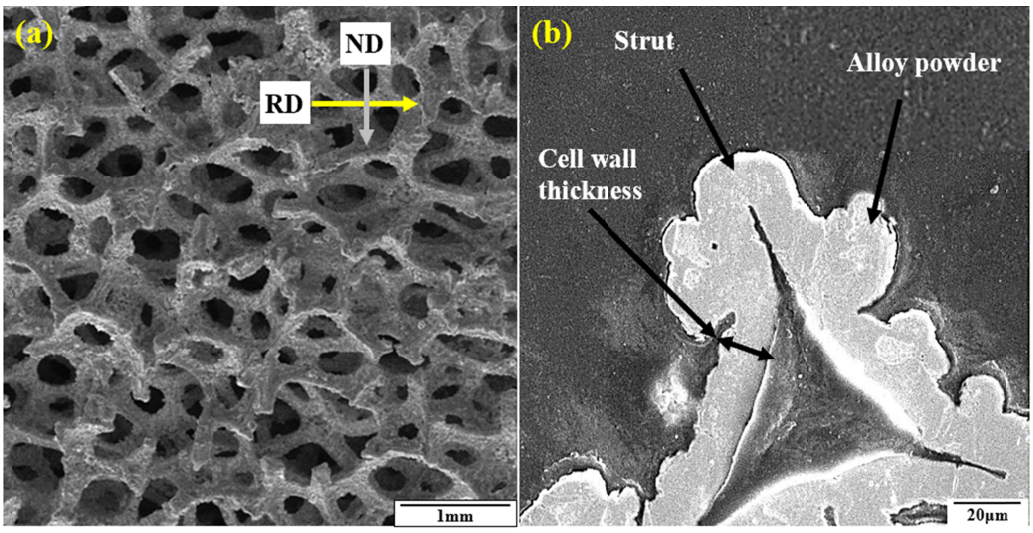

Fig. 2. SEM images for (a) pore structure, (b) cross-section of strut of Ni-Cr-Al powder porous metal

which was measured and compared from different directions, measured 1161 μm, 1030 μm and 960 μm in the RD, TD and ND direction, respectively. The average strut thickness was 132 μm, and cell wall thickness was 18.7 μm. As the porous metal above was manufactured by stacking sheet foam and then applying rolling, the compression caused the pores to elongate in the ND direction. The relative density of the cubic-shaped Ni-Cr-Al porous metal measured 6.72%. Fig. 2(b) is the cross-sectional, microstructural observation result of the strut that influenced the mechanical properties of porous metals. The strut's interior had a triangular void that was formed due to the polyurethane pre-form used during the manufacturing of the material that was removed by heat treatment. In addition, it was also possible to find sprayed powder adhered to the strut surface.

Fig. 3 shows the XRD analysis result of Ni-Cr-Al powder porous metal and observations results of the etched microstructure. In the XRD analysis (a), the porous metal had γ-Ni and γ'-Ni_3Al peaks. In the microstructure and EDS analysis results, γ'-Ni_3Al was found. Alloy element analysis of the strut cross section (Fig. 3(c)) confirmed that Ni, Cr and Al elements were evenly distributed on the cell wall and alloying powder. Based on such findings, it is possible to suspect that Ni matrix, γ'-Ni_3Al are relatively evenly distributed in both the strut and adhered powder. When manufacturing a Ni-Cr-Al porous metal, sintering and homogenization occur simultaneously according to the heat treatment after spraying alloy powder, and such result in the even distribution.

Fig. 4 depicts compression test results of Ni-Cr-Al porous metal at room temperature and 800°C in ND and RD directions. As shown in the figure, the compression curve of the cubic-shaped powder porous metal can be categorized as a typical open foam which is composed of three compression behavior areas, elastic, plateau and densification. Based on the ND and RD room temperature compression test result, the compressive yield strength measured 0.95 MPa and 1.35 MPa, respectively. In the case of RD, the compressive yield strength and plateau strength measured high. In the case of ND compression, a flat plateau area was measured short, and the stress increased sharply. However, RD did not show a clear plateau area, and as strain increased, the compressive stress increased with a gradual curve. With such differences it was possible to identify the mechanical anisotropy of the powder porous metal used in this study. It is known that the anisotropy of porous materials is influenced by the pore's morphology [12-14]. As described in Fig. 2, the cubic-shaped Ni-Cr-Al porous metal was manufactured by stacking porous metal sheets and compressing them. Therefore, elongated pores and bonding areas between sheets resulted in the occurrence of clear anisotropy. Fig. 4 (c) and (d) show the deformation and fracture behaviors of the specimen after compression. It was possible to identify that pores were collapsed in the specimen compressed in the ND direction (white arrow). If the elongation direction of pores and compressive direction are perpendicular (ND), fracture occurs at low stress levels as stress concentration occurs on nodes as stress increases. Meanwhile, in the case of RD, which is the elongated direction pores and compressive direction are parallel, buckling can be easily formed due to bending stress applied on the strut (yellow arrow). The high temperature compression properties of the powder porous metal are lower compared to room temperature conditions, but in general, they had similar characteristics. In high temperature conditions, the ND and RD compressive yield strengths measured 0.44 MPa and 0.76 MPa, respectively. Something to note was that there was

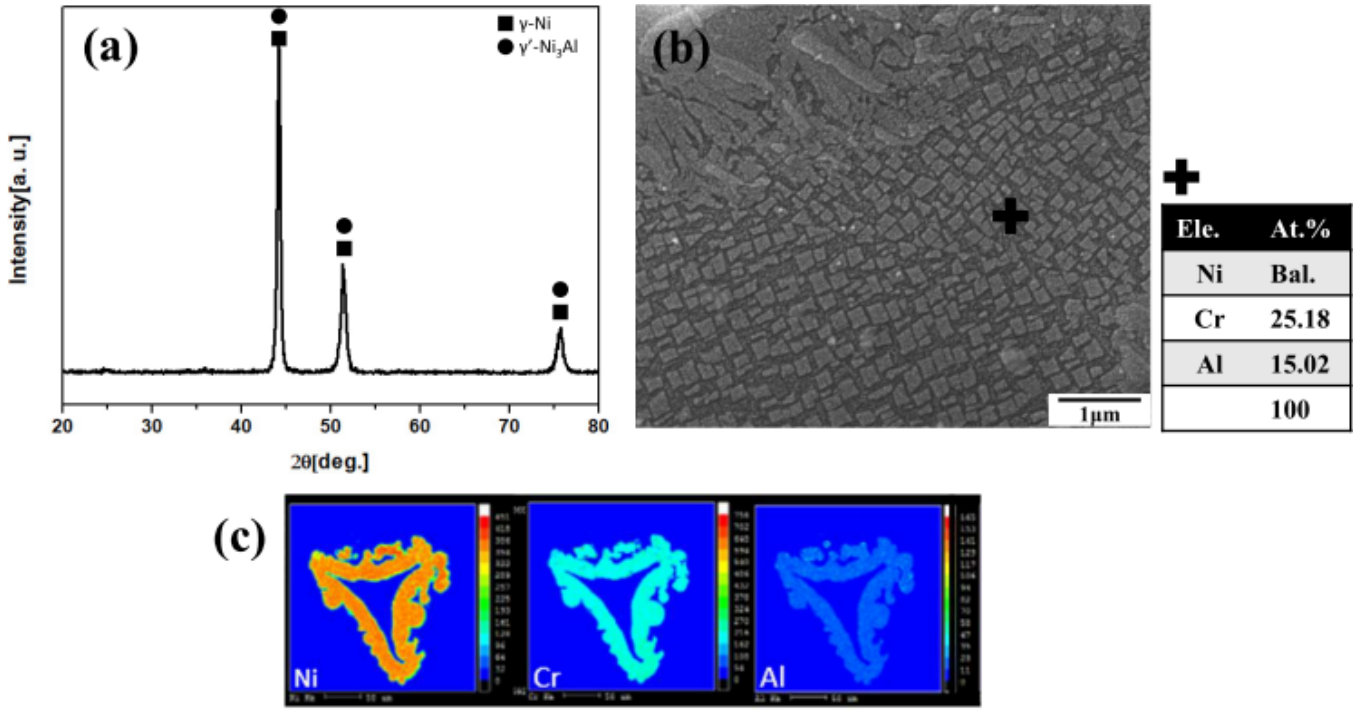

Fig. 3. Results of phase analysis and images of microstructure (a) X-ray diffraction analysis, (b) SEM image of γ'-phase, and (c) EPMA images of cross-section of Ni-Cr-Al powder porous metal

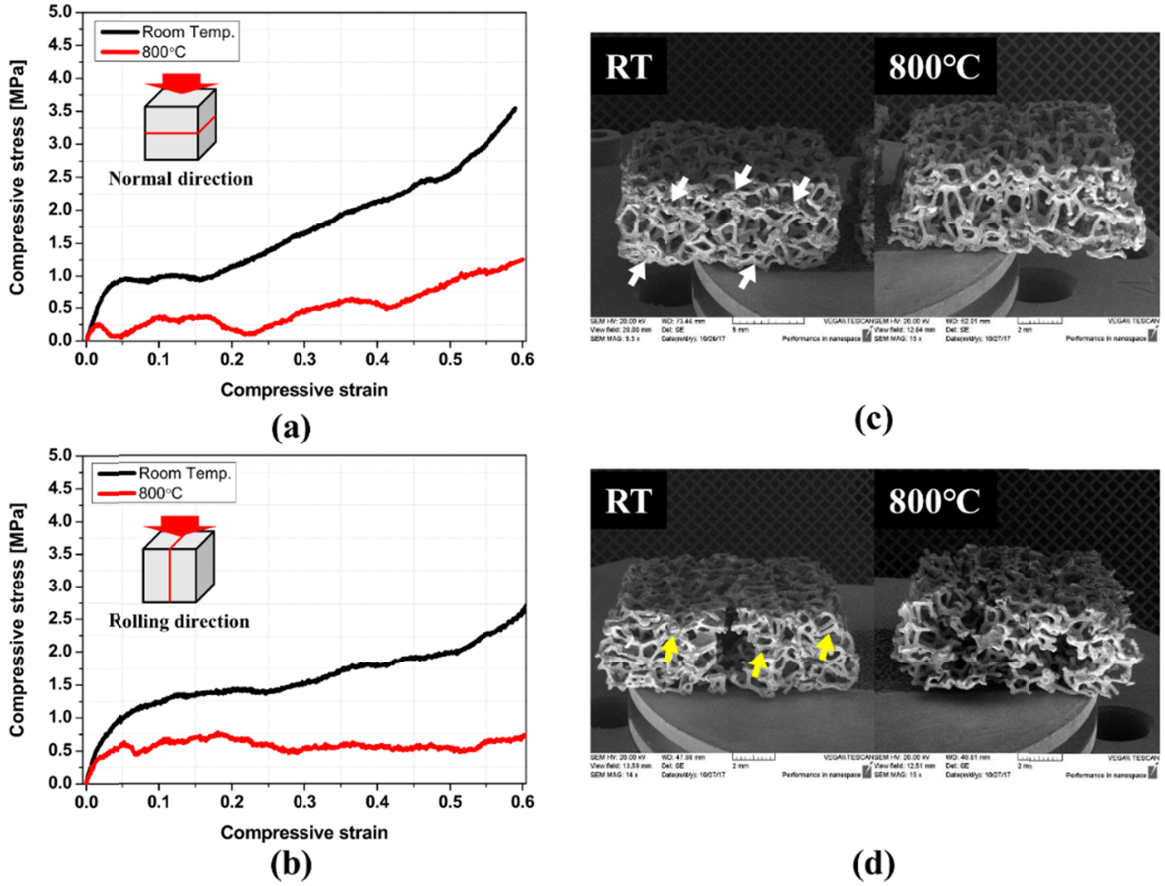

Fig. 4. Compressive stress vs. strain curves at room and 800°C temperatures with different directions and macro images after compression tests with temperatures (a) normal direction (ND), (b) rolling direction (RD), macro images of ND compressed specimens, and (d) macro images of RD compressed specimens

a section where stress decreased in the ND (red arrow). This is suspected to be due to the non-continuous pore collapse after elastic behavior [1].

Fig. 5 shows the creep strain vs. time curves obtained from the random stack creep tests. In all curves, it is possible to see primary creep and secondary creep behaviors. Creep strain measured 8.09×10^{-5}, 7.66×10^{-4}, 0.07, 0.43 and 0.48 respectively starting from low stress. Something to note is that the strain increased significantly at loads greater than 0.228 MPa. In order to identify the cause of this, the volume according to the stacking height of the specimen was calculated, and this was divided by the mass of 16 specimens to calculate the relative density of powder porous metals in the creep jig. As a result, the relative density of porous metal before the test was 3.17% on average. This means that there are more spaces between the cubic-shaped porous metals (compared to cubic porous metal itself). After creep deformation from 0.114 MPa to 0.38 MPa, the relative density change measured as 3.22% (0.114 MPa), 3.27% (0.152 MPa), 3.42% (0.228 MPa), 5.57% (0.304 MPa) and 6.11% (0.380 MPa), respectively. The reason the initial primary creep amount has a large change with applied stress can be interpreted to be due to the voids between the randomly stacked cubes decreasing significantly according to stress. A unique behavior with greater initial creep strain of randomly stacked cubes compared to a single porous metal can be understood.

In order to quantify creep behavior, the creep time-strain relationship was analyzed using the following equation presented by Dorn and Galofalo et al. [13-14].

$$\varepsilon = \varepsilon_0 + \varepsilon_t(1-e^{-rt}) + \dot{\varepsilon}_{ss}t \tag{1}$$

Where, ε_0 is the instantaneous strain, r is the ratio between transient creep rate and transient creep strain, ε_t is the total transient strain, $\dot{\varepsilon}_{ss}$ is the steady-state creep rate, and t is the time. In addition, it is possible to linearize the secondary creep rate according to stress by using the following relationship of Sherby-Dorn equation.

$$\dot{\varepsilon}_{ss} = A\sigma^n \exp\left(\frac{-Q}{RT}\right) \tag{2}$$

Where Q is the activation energy of creep, A is the material parameter, T is the absolute temperature, σ is the additional stress, n is the stress exponent, and R is the ideal gas constant. Fig. 6 shows the secondary creep rate and creep exponent calculated using (1) and (2). The steady state creep rate had a very low value in approximately the 1E-10 range. This is lower by two orders compared to other study results using similar relative density [12]. In addition, from the stress range (~0.152 MPa) which had a relatively lower creep strain than 0.224 MPa had n = 1.6, and at higher stress range n = 0.4. In other words, at higher stress, the creep exponent was smaller than 1, indicating that it is rela-

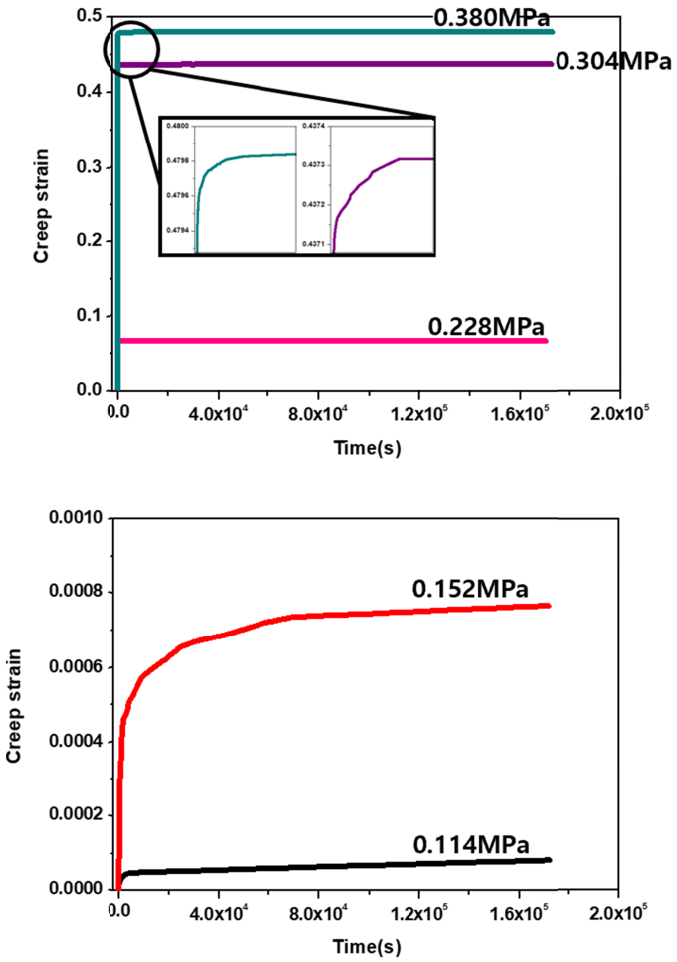

Fig. 5. High temperature random stack creep curves of Ni-Cr-Al powder porous metal

tively less sensitive to stress. In general, diffusion creep behavior is known to occur in bulk materials when n = 1 [15-16]. The reason such a result is obtained is suspected to be due to i) the cell morphology of the porous metal, and ii) the characteristics of the random stack creep condition. The porous material must be considered to have a structure similar to a cell morphology composed of pores and struts that make up pores. In particular,

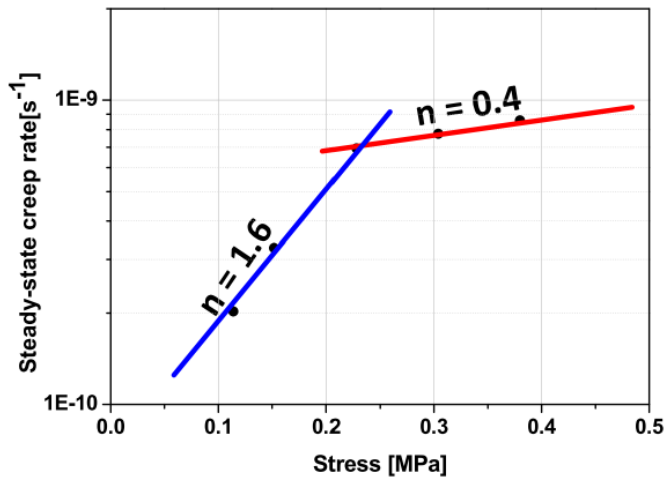

Fig. 6. Stress dependence of the secondary creep rate of the Ni-Cr-Al powder porous metal at 800°C

the random creep test can cause significant deformation due to the additional voids created by the irregular stacking of cubic foams. This can be deducted from most of the strains occurring in the primary creep area of the creep time vs. strain curve and from the change in relative density of the powder porous specimen. This causes densification in the random staked specimens, which leads to the condition that the actual specimen is in a low stress condition. Therefore, the random stacked powder porous specimens represent unique creep properties of low creep strain rate and low creep stress exponent.

4. Conclusion

This study investigated high temperature random stack creep properties using Ni-Cr-Al powder porous metal in actual application environments, and came to the following conclusion: The Ni-Cr-Al porous metal had a pore size of 1161 μm (RD), strut thickness of 132 μm, and relative density of 6.72%. Initial microstructural observation identified γ and γ' phases. EPMA analysis results confirmed that alloy elements are evenly distributed throughout the material after spraying alloy powder. The room temperature and high temperature compression results showed characteristics of a typical compression curve. In addition, it showed anisotropy in each compressive direction. High temperature random stack creep results confirmed different limits for transient creep strain (ε_t) in different stress ranges. Along with this, a steady creep rate of ~10^{-10} sec.$^{-1}$ (<10^{-9} sec^{-1}) was obtained from all stress ranges. This creep rate is significantly lower than the creep rate obtained from single powder porous metal. This can be explained to be caused by the porous structure densification occurring in the primary creep area.

Acknowledgments

This study was supported by Program for the Development of Strategic Core Materials, Republic of Korea government ministry of Trade, Industry and Energy.

REFERENCES

[1] L.J. Gibson and M.F. Ashby, Cellular solids: Structure and Properties, 2nd Ed. Cambridge University Press, 1997.
[2] M.F. Ashby, A.G. Evans, N.A. Fleck, L.J. Gibson, J.W. Hutchinson and H.N.G. Wadley, Metal Foams: A design Guide, Oxford, 2000.
[3] Wadley HNG, Cellular metals and metal foaming technology, Verlag MIT, 2001.
[4] G.J. Davies, Shu Zhen, Jour. Mater. Sci. **18**, 1899 (1983).
[5] A.M. Hodge, D.C. Dunand, Intermetallics **9**, 581 (2001).
[6] D.T. Queheillalt, Y. Katsumura, H.N.G. Wadley, J. Mater. Res. **16**, 1028 (2001).
[7] Y. Boonyongmaneeratand, D. C. Dunand, Adv. Eng. Mater. **10** (4), 379 (2008).

[8] L. Murr, S. Li, Y. Tian, K. Amato, E. Martinez, F. Medina, Materials **4** (4), 782 (2011).

[9] G. Walther, B. Kloden, T. Buttner, T. Weissgarber, B. Kieback, A. Bohm, D. Naumann, S. Saberi, L. Timberg, Adv. Eng. Mater. **10**, 803 (2008).

[10] B.H. Kang, M.H. Park, K.A. Lee, Arch. Metall. Mater. **62**, 2(B), 1329 (2017).

[11] K.S. Kim, J.Y. Yun, B.G. Choi, K.A. Lee, Met. Mater. Int. **20**, 507 (2014).

[12] L. Giani, G. Groppi, E. Tronconi, Ind. Eng. Chem. Res. **44**, 4993 (2005).

[13] K.E. Amin, A.K. Mukherjee, J.E. Dorn, J. Mech. Phys. Solids **18**, 413 (1970).

[14] G.A. Webster, A.P.D. Cox, J.E. Dorn, Metal Sci. J. **3**, 221 (1969).

[15] J. RÖsler, R. Joos, E. Arzt, Met. Trans. A **23A**, 1521 (1992).

[16] O.D. Sherby, G. Gonzalez-Doncel, O.A. Ruano, Threshold stresses in particle-hardened materials, Creep and fracture of engineering materials and structures, J.C. Earthman and F.A. Mohamed (eds), TMS, 1997, pp. 9-18.